Research Square

Preprints are preliminary reports that have not undergone peer review.
They should not be considered conclusive, used to inform clinical practice,
or referenced by the media as validated information.

Central Atom Effects in ZnPc-Based HTMs: A DFT/TD-DFT Study for Solar Cell Applications

Mustapha Ammari

mu.ammari@edu.umi.ac.ma

University Moulay Ismail of Meknes

Mohamed Jabha

University of Moulay Ismail of Meknès

Mohamed YAAKOUBI

University of Moulay Ismail of Meknès

Nazih Asoufar

University of Moulay Ismail of Meknès

Abdellah Elalaoui

University Moulay Ismail of Meknes

El Houssine Mabrouk

University of Moulay Ismail of Meknès

Research Article

Keywords: DFT/TD-DFT, B3LYP/6-311G(d,p) /LANL2DZ, phthalocyanine derivatives, central atom effect, hole-transport materials (HTMs), perovskite solar cells

Posted Date: November 18th, 2026

DOI: https://doi.org/10.21203/rs.3.rs-11492637/v1

License: This work is licensed under a Creative Commons Attribution 4.0 International License.
Read Full License

Additional Declarations: No competing interests reported.

Central Atom Effects in ZnPc-Based HTMs: A DFT/TD-DFT Study for Solar Cell Applications

Mustapha Ammari* [a], Mohamed Jabha [b], Mohamed YAAKOUBI [b], Nazih Asoufar [b], Abdellah Elalaoui [a], El Houssine Mabrouk [b]

[a] Crystalline Materials and Engineering team, Faculty of Sciences, University Moulay Ismail of Meknes, Meknes, Morocco

[b] Laboratory of Materials Engineering for the Environment and Natural Ressources, Faculty of Sciences and Techniques,University of Moulay Ismail of Meknès, Errachidia, Morocco

Corresponding Author E-mail: mu.ammari@edu.umi.ac.ma

Abstract

This study aims to analyze how the central atom affects the structural, electronic, and optical properties of nine phthalocyanine derivatives (Zn-Pc, Cu-Pc, Cd-Pc, C-Pc, Si-Pc, Ge-Pc, S-Pc, Se-Pc, and Te-Pc) used as hole-transport materials (HTMs) in perovskite solar cells. The molecules were optimized using density functional theory (DFT), while UV–Visible absorption properties were investigated using TD-DFT method. The results show that the central atom influences the bond lengths, molecular geometry, charge distribution, and electronic properties of the derivatives. Frontier molecular orbital analysis reveals HOMO delocalization, which facilitates hole transport. The strongest absorption bands were observed for Zn-Pc, Cu-Pc, and Cd-Pc, whereas Ge-Pc, S-Pc, and Se-Pc exhibited intermediate intensities. C-Pc, Si-Pc, and Te-Pc showed weak absorption in the visible region, with the absorption band of Te-Pc shifted toward the near-infrared region. These results indicate that C-Pc, Si-Pc, and Te-Pc are the most suitable candidates as HTMs in perovskite solar cells.

Keywords: DFT/TD-DFT; B3LYP/6-311G(d,p) /LANL2DZ; phthalocyanine derivatives; central atom effect; hole-transport materials (HTMs); perovskite solar cells.

1. Introduction

Renewable energy is receiving increasing attention because it helps reduce pollution and meet the growing energy demand [1]. Alternative energy sources must be efficient, affordable, and environmentally friendly. In this context, using solar energy is a good option because the amount of sunlight received by the Earth each day is far greater than the world's annual energy demand. Consequently, a photovoltaic installation with a moderate efficiency of 8–10% and occupying a limited area of the Earth could generate a significant amount of electrical energy, thereby contributing to the reduction of greenhouse gas emissions.

These considerations have encouraged the emergence of innovative photovoltaic technologies, including organic photovoltaic cells (OPVs), dye-sensitized solar cells (DSSCs), perovskite solar cells (PSCs), and quantum-dot solar cells (QDSCs), which represent third-generation photovoltaic technologies [2] [3] [4] [5].

Due to their exceptional electrical, mechanical, magnetic, and optical properties, perovskite solar cells (PSCs) have made significant progress over the past decade [6] [7]. Among the most promising emerging photovoltaic technologies, organic–inorganic hybrid perovskite solar cells reached a decisive milestone in 2012. At that time, research teams led by Park and Smith independently demonstrated the effectiveness of an organic material, 2,2′,7,7′-tetrakis(N,N-di-p-methoxyphenylamine)-9,9′-spirobifluorene (spiro-OMeTAD), used as a hole-transport material (HTM) in perovskite solar cells. The hole-transport material (HTM) was initially used in conjunction with a liquid electrolyte. This advance significantly contributed to improving the performance of perovskite solar cells [8] [9]. Since then, spiro-OMeTAD has established itself as one of the most widely used hole-transport materials (HTMs) in state-of-the-art n-i-p architectures, particularly because of its significant contribution to achieving high photovoltaic efficiencies and outstanding performance [10].

Understanding how molecular structure affects electronic properties is important for developing new efficient hole-transport materials (HTMs) for perovskite solar cells [11]. Theoretical and experimental approaches make it possible to evaluate key parameters such as the energy gap and HOMO/LUMO levels, which play a determining role in the properties and photovoltaic performance of the materials [12].

Density functional theory (DFT) is a reliable approach for analyzing the structural, electronic, and optical properties of molecular systems. In the present work, zinc phthalocyanine (ZnPc) and a series of derivatives obtained by substituting the central Zn atom with different elements (Cu, Cd, C, Si, Ge, Se, S, and Te) are investigated theoretically. This study aims to highlight the influence of the nature of the central atom on the structural, electronic, and optical properties of the phthalocyanine derivatives, as well as to evaluate the potential of these derivatives as hole-transport materials (HTMs) for perovskite solar cells.

2.Computational methodology

Density functional theory (DFT) calculations were performed using the B3LYP functional and the 6-311G(d,p) and LANL2DZ basis sets [13] to optimize the geometries of the phthalocyanine derivatives in the ground state. The optimized structures were visualized using GaussView 6.0 [14]. The optimized structures are presented in Figure 1. The central zinc atom was substituted with elements from various groups of the periodic table, including Group 14 elements (carbon, silicon, and germanium), transition metals (copper and cadmium), and chalcogens (sulfur, selenium, and tellurium), in order to evaluate the impact of the nature of the central atom on the structural, electronic, and optical properties of the analyzed phthalocyanines.

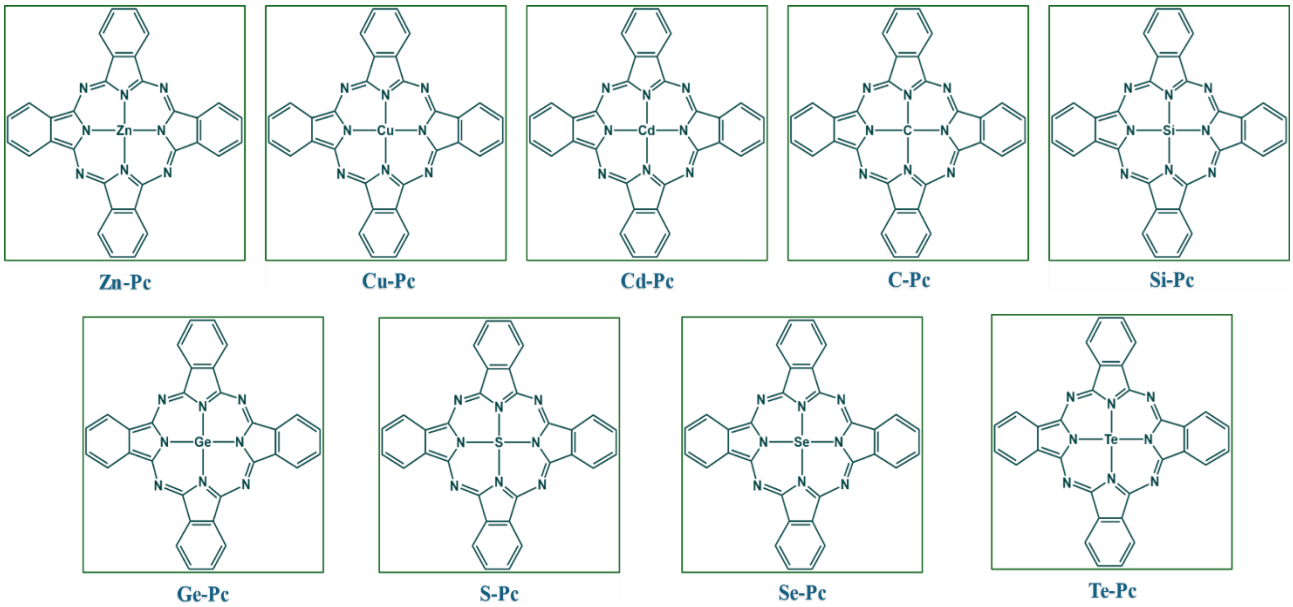


Fig. 1. Representation of the molecular structures of ZnPc and its derivatives investigated by substitution of the central Zn atom.

3. Results and discussion

3.1 Geometry parameters

Figure 2 illustrates the optimized geometries of nine phthalocyanine derivatives (Zn-Pc, Cu-Pc, Cd-Pc, C-Pc, Si-Pc, Ge-Pc, S-Pc, Se-Pc, and Te-Pc), obtained using DFT at the B3LYP/LANL2DZ level [15], [16]. We study the geometrical parameters because they provide information about how the central atom influences the molecular structure, which can in turn influence the electronic properties of the HTMs. The geometrical parameters are summarized in Table 1. We observe that the distance between the central atom and the coordinating nitrogen atoms, M–N, varies from approximately 1.4 to 1.9 Å for Zn-Pc, C-Pc, Cu-Pc, and Si-Pc, whereas it ranges from approximately 2.03 to 2.17 Å for Ge-Pc, Cd-Pc, Te-Pc, Se-Pc, and S-Pc. Regarding the N–M–N angles, most derivatives exhibit values close to 90°, indicating a central geometry close to planarity. However, C-Pc and Ge-Pc exhibit angles of 103.788° and 79.485°, respectively, suggesting a greater deformation of the structure around the central atom. Finally, for the C–N bond lengths, we observe small variations among the different compounds [17].

Table 1. Analysis of the representative geometrical parameters of the optimized structures of ZnPc and the investigated phthalocyanine derivatives.

Parameter	ZnPc	C-Pc	Cu-Pc	Si-Pc	Ge-Pc	Cd-Pc	Te-Pc	Se-Pc	S-Pc
Distance M–N (Å)	1.99664	1.483	1.976	1.780	2.170	2.118	2.174	2.085	2.034
N–M–N angle (°)	90.005	103.788	90.000	91.857	79.485	90.003	90.000	90.000	90.000
C–N bond length (Å)	1.369	1.400	1.393	1.416	1.373	1.385	1.377	1.359	1.361

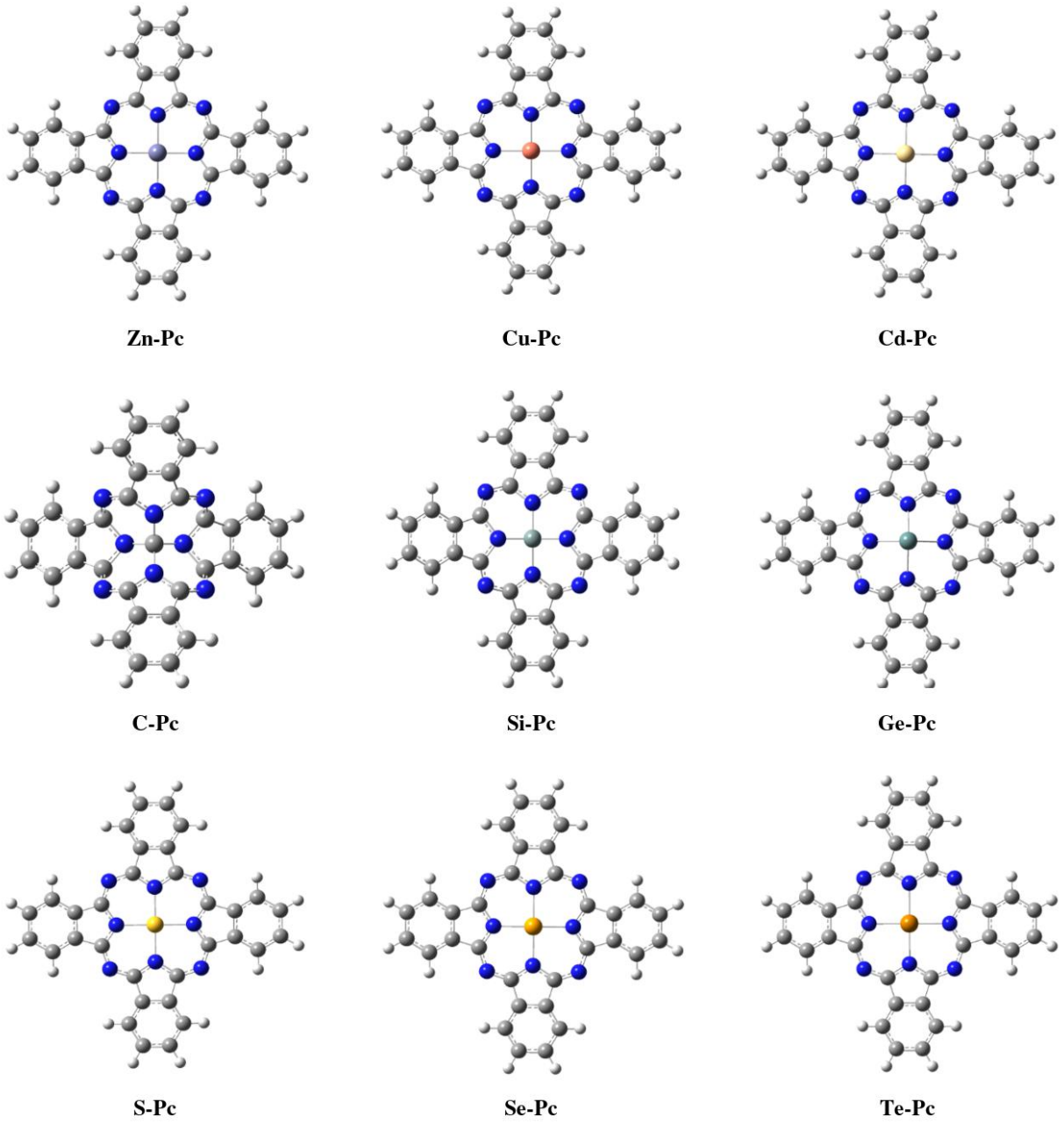


Fig. 2. Optimized structures of ZnPc and the investigated phthalocyanine compounds obtained by substitution of the central Zn atom.

3.2. Frontier molecular orbital (FMO)

Figure 3 shows the distribution of the HOMO and LUMO orbitals of the nine phthalocyanine derivatives studied ((a) Zn-Pc, (b) Cu-Pc, (c) Cd-Pc, (d) C-Pc, (e) Si-Pc, (f) Ge-Pc, (g) S-Pc, (h) Se-Pc, and (i) Te-Pc). This representation makes it possible to analyze their electronic structure and the influence of the central atom on the distribution of electron density [25]. These orbitals

also make it possible to fine-tune the electronic structure and the photophysical and electrochemical properties [18][19], [20] Based on our observations, We can say that the studied structures show a relatively extended distribution of electron density associated with the HOMO, which covers the whole molecule. A similar trend is seen for the electron density related to the LUMO, though it is more strongly focused in the areas with nitrogen atoms. The electron density associated with the HOMO thus seems to be more widely distributed than that associated with the LUMO for all the derivatives studied. For Se-Pc and Te-Pc, however, we observe that the electron-density distributions of the HOMO and LUMO also spread into the molecule's central region.[21][22][23]. This strong delocalization promotes charge-carrier mobility and improves hole transport, an essential criterion for hole-transport materials (HTMs) intended for perovskite solar cells [24].

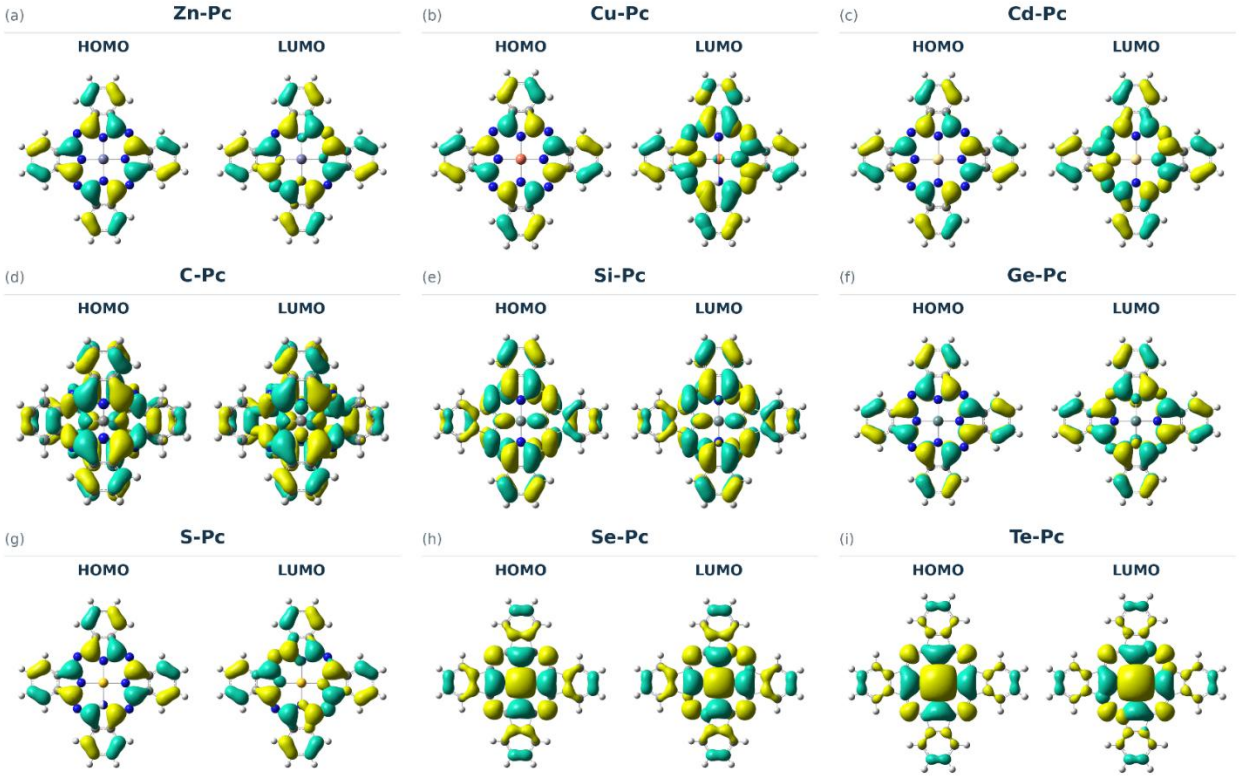


Fig. 3. HOMO and LUMO surface plots of (a) Zn-Pc, (b) Cu-Pc, (c) Cd-Pc, (d) C-Pc, (e) Si-Pc, (f) Ge-Pc, (g) S-Pc, (h) Se-Pc, and (i) Te-Pc.

3.3 Molecular Electrostatic Potential (MEP)

Electrostatic potential (ESP) maps help visualize how electron density is distributed in the materials [25][26]. This charge distribution is essential for the electronic and photovoltaic properties, particularly the current density and the efficiency of photovoltaic devices [27]. Regions of high electronegativity in the molecules are shown in red, whereas electropositive parts are indicated in yellow, and regions of high electropositivity are shown in blue. Analysis of the ESP maps reveals the presence of moderately electropositive regions, represented in yellow. Figure 4 presents the electrostatic potential (ESP) maps of all the molecules studied.

Among the molecules studied, with the exception of Te-Pc, the Zn-Pc, Cd-Pc, and Si-Pc compounds are distinguished by a strongly electropositive blue region around the central atom, whereas S-Pc and Se-Pc exhibit a strongly electronegative red central region. For the other molecules, the center is predominantly yellow. In addition, the peripheral regions of S-Pc, Se-Pc, C-Pc, Ge-Pc, Cd-Pc, and Cu-Pc, shown in red, correspond to highly electronegative regions [28][29][30]. The observed variations among the derivatives show that replacing the metal changes the magnitude and distribution of the electrostatic potential, which may therefore influence intermolecular interactions.

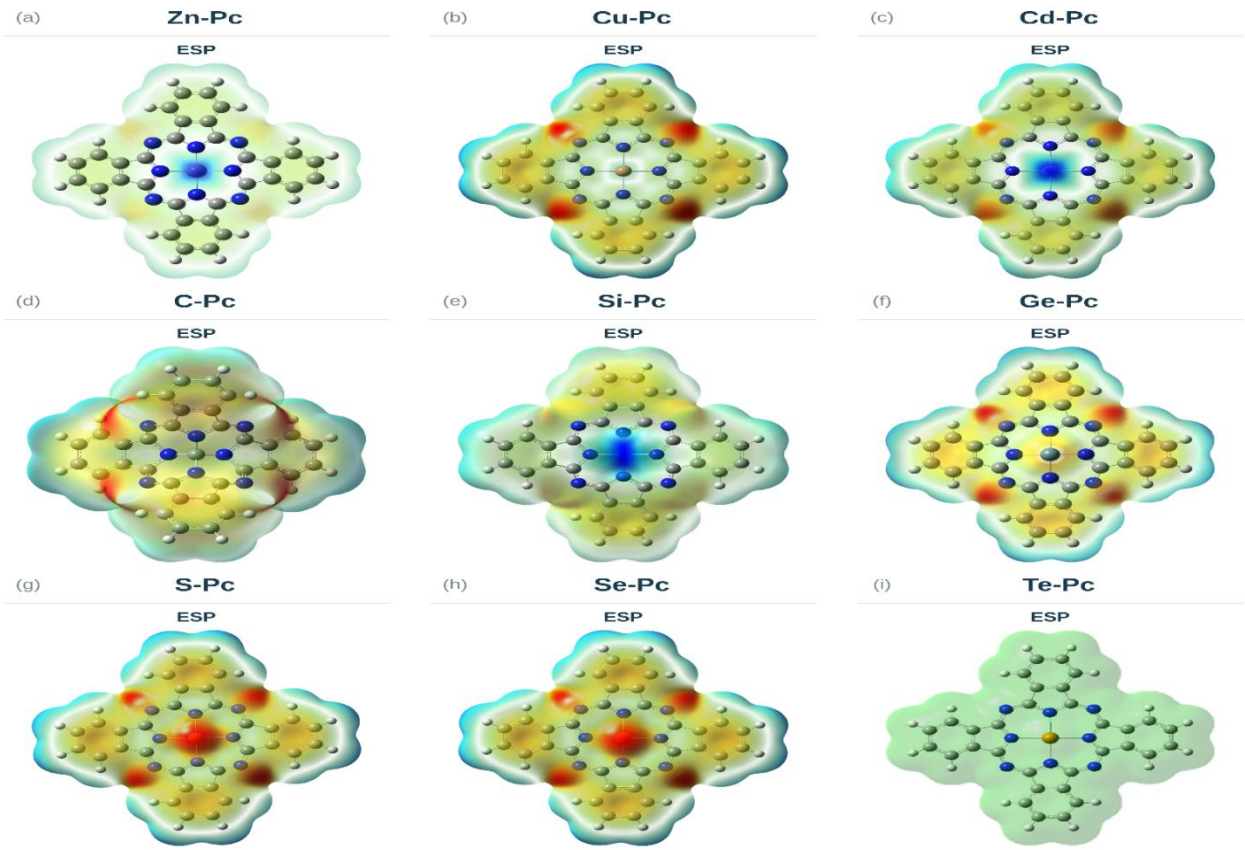


Fig. 4. Molecular electrostatic potential maps of the studied hole-transport materials: (a) Zn-Pc, (b) Cu-Pc, (c) Cd-Pc, (d) C-Pc, (e) Si-Pc, (f) Ge-Pc, (g) S-Pc, (h) Se-Pc, and (i) Te-Pc.

3.4 Bandgap energy

The calculated HOMO and LUMO levels are presented in Table 2. We found that the HOMO energy levels of Zn-Pc, Cu-Pc, Ge-Pc, Se-Pc, S-Pc, and Cd-Pc lie between −5.0 and −5.4 eV, which is suitable for $MAPbI_3$ perovskite, whose valence band is located around −5.4 eV figure 5. We also observe that the LUMO levels of all HTMs are above the conduction-band minimum of $MAPbI_3$ [31], [32]. This helps prevent an excited electron promoted from the valence band (VB) to the conduction band (CB) of the perovskite from being transferred to the LUMO level of the HTM instead of reaching the conduction band of the electron-transport material. We also found that all HTMs have an energy gap greater than 2 eV, except for Si-Pc and Te-Pc, which exhibit values of 1.382 and 1.327 eV, respectively.

Table 2. Frontier molecular orbital energies (HOMO and LUMO) and energy gaps of the investigated phthalocyanine derivatives.

	E_{HOMO} (eV)	E_{LUMO} (eV)	Eg (eV)
C-PC	**-4.711**	**-2.645**	**2,066**
Si-PC	**-4.400**	**-3.018**	**1,382**
Ge-PC	**-5.196**	**-3.103**	**2,093**
S-Pc	**-5.294**	**-3.156**	**2,138**
Se-Pc	**-5.227**	**-3.197**	**2,030**
Te-Pc	**−4.688**	**−3.361**	**1.327**
Cd-PC	**-5.366**	**−3,167**	**2,199**
Cu-Pc	**−5,326**	**−3,131**	**2,195**
Zn-Pc	**−5,161**	**−2,983**	**2,178**

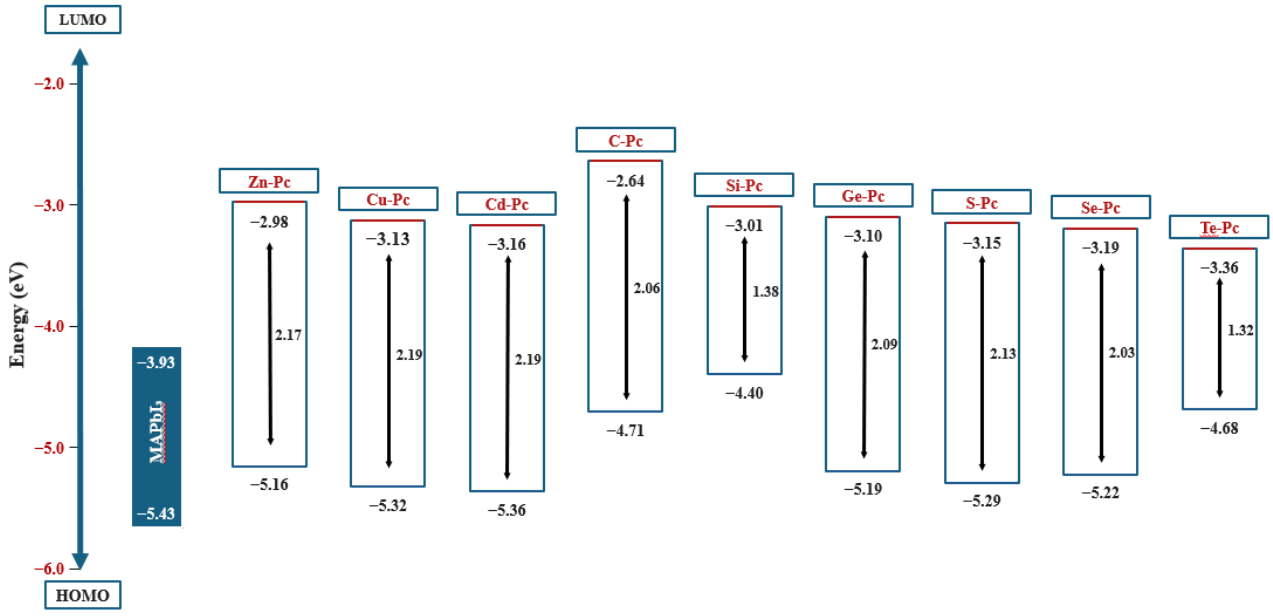


Fig. 5. Frontier energy-level alignment of the investigated phthalocyanine-based hole-transporting materials (HTMs) with $MAPbI_3$.

3.5 Electronic Parameters (IP, EA, χ, η, ω, S, N)

We calculated the ionization potential (IP), electron affinity (EA), electronegativity (χ), chemical hardness (η), electrophilicity index (ω), chemical softness (S), and number of transferred electrons (N) of the investigated phthalocyanine compounds using the following equations [33], [34], [35], [36].

$$(1)\ IP = -E_{HOMO}$$

$$(2)\ EA = -E_{LUMO}$$

$$(3)\quad \chi = \frac{IP+EA}{2}$$

$$(4)\quad \eta = \frac{IP-EA}{2}$$

$$S = \frac{1}{2\eta} \quad (5)$$

$$\omega = \frac{\mu^2}{2\eta} \quad (6)$$

$$\Delta N_{max} = \frac{\chi}{\eta} \quad (7)$$

The results obtained are summarized in Table 3 and figure 6. We observe that substitution of the central atom clearly modifies the electronic properties of the phthalocyanines. Si-Pc and Te-Pc exhibit the lowest ionization potentials and chemical hardness values, as well as the highest softness values, which facilitates their polarization and charge transfer [37], [38], [39]. In contrast, CuPc, Cd-Pc, and ZnPc are more stable but less reactive. Te-Pc and Si-Pc therefore appear to be the most promising candidates, subject to suitable energy-level alignment with the perovskite.

[Insert Table 3 here]

Table 3. Calculated electronic reactivity parameters (IP, EA, χ, η, ω, S, and N) of the investigated phthalocyanine compounds.

Compound	IP (eV)	EA (eV)	χ (eV)	η (eV)	ω (eV)	S (eV^{-1})	N
C-Pc	**4,711**	**2,645**	**3,678**	**1,033**	**6,548**	**0,968**	**3,561**
Si-Pc	**4,400**	**3,018**	**3,709**	**0,691**	**9,954**	**1,447**	**5,368**
Ge-Pc	**5,196**	**3,103**	**4,150**	**1,047**	**8,227**	**0,956**	**3,965**
S-Pc	**5,294**	**3,156**	**4,225**	**1,069**	**8,349**	**0,935**	**3,952**
Se-Pc	**5,227**	**3,197**	**4,212**	**1,015**	**8,739**	**0,985**	**4,150**
Te-Pc	**4,688**	**3,361**	**4,025**	**0,664**	**12,205**	**1,507**	**6,066**
Cd-Pc	**5,366**	**3,167**	**4,267**	**1,100**	**8,278**	**0,910**	**3,880**
Cu-Pc	**5,326**	**3,131**	**4,229**	**1,098**	**8,146**	**0,911**	**3,853**
Zn-Pc	**5,161**	**2,983**	**4,072**	**1,089**	**7,613**	**0,918**	**3,739**

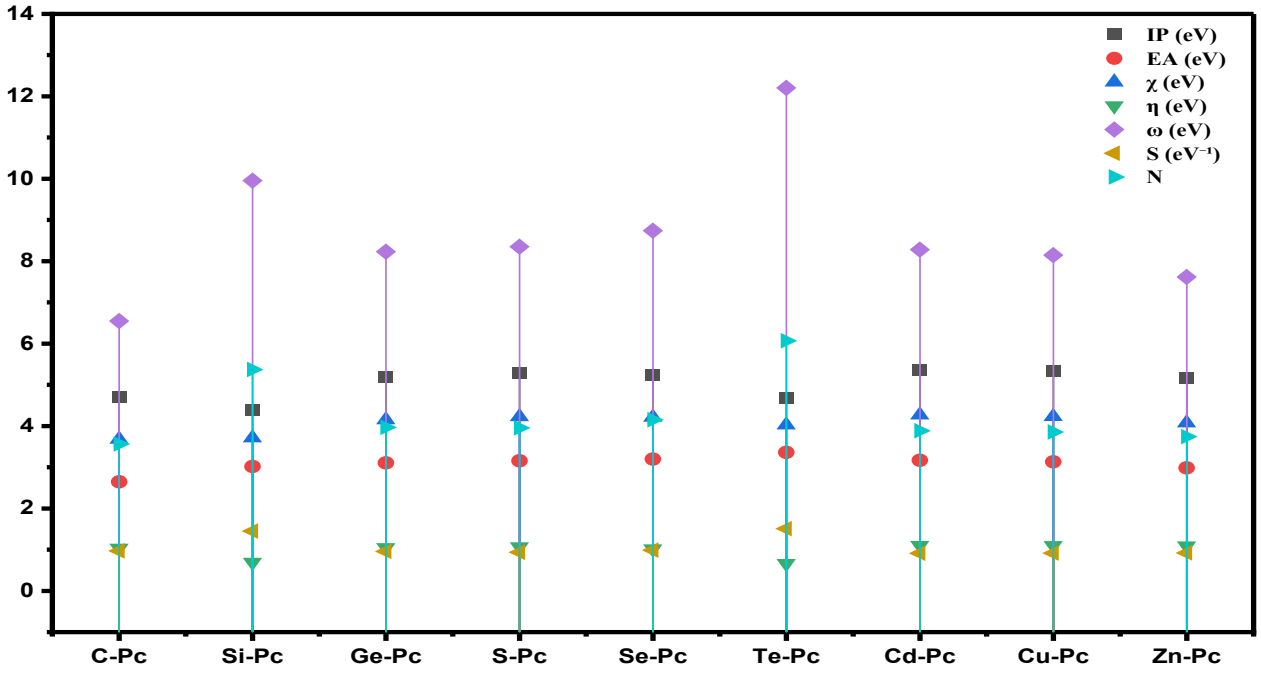


Fig. 6. Comparison of the calculated electronic reactivity parameters (IP, EA, χ, η, ω, S, and N) for the investigated phthalocyanine compounds.

3.6 Non-Covalent Interaction Analysis

We performed an NCI-RDG analysis to identify the noncovalent interactions present in the studied molecules [40], [41]. This analysis allowed us to distinguish attractive interactions. Negative values of sign(λ_2)ρ indicate attractive interactions, whereas positive values reveal repulsive interactions [42], [43]. The green regions at the centers of the aromatic rings and around the macrocycle mainly indicate weak van der Waals interactions. The red and orange regions located near the central atom and in certain cavities indicate repulsive interactions between atoms [44]. It can be observed that, in Ge-Pc, Si-Pc, and Te-Pc, the NCI surfaces located around the central atom are more extended, showing that the nature of this atom influences the distribution of interactions in this region. In Cd-Pc, Cu-Pc, and Zn-Pc, the repulsive zones are more localized around the metal center. The green surfaces and the peaks located near sign(λ_2)$\rho \approx 0$ indicate a predominance of weak van der Waals interactions. In contrast, the red regions associated with positive values mainly correspond to steric effects [45]. The RDG scatter plots and NCI isosurfaces are presented in Fig. 7.

[Insert Fig. 7 here]

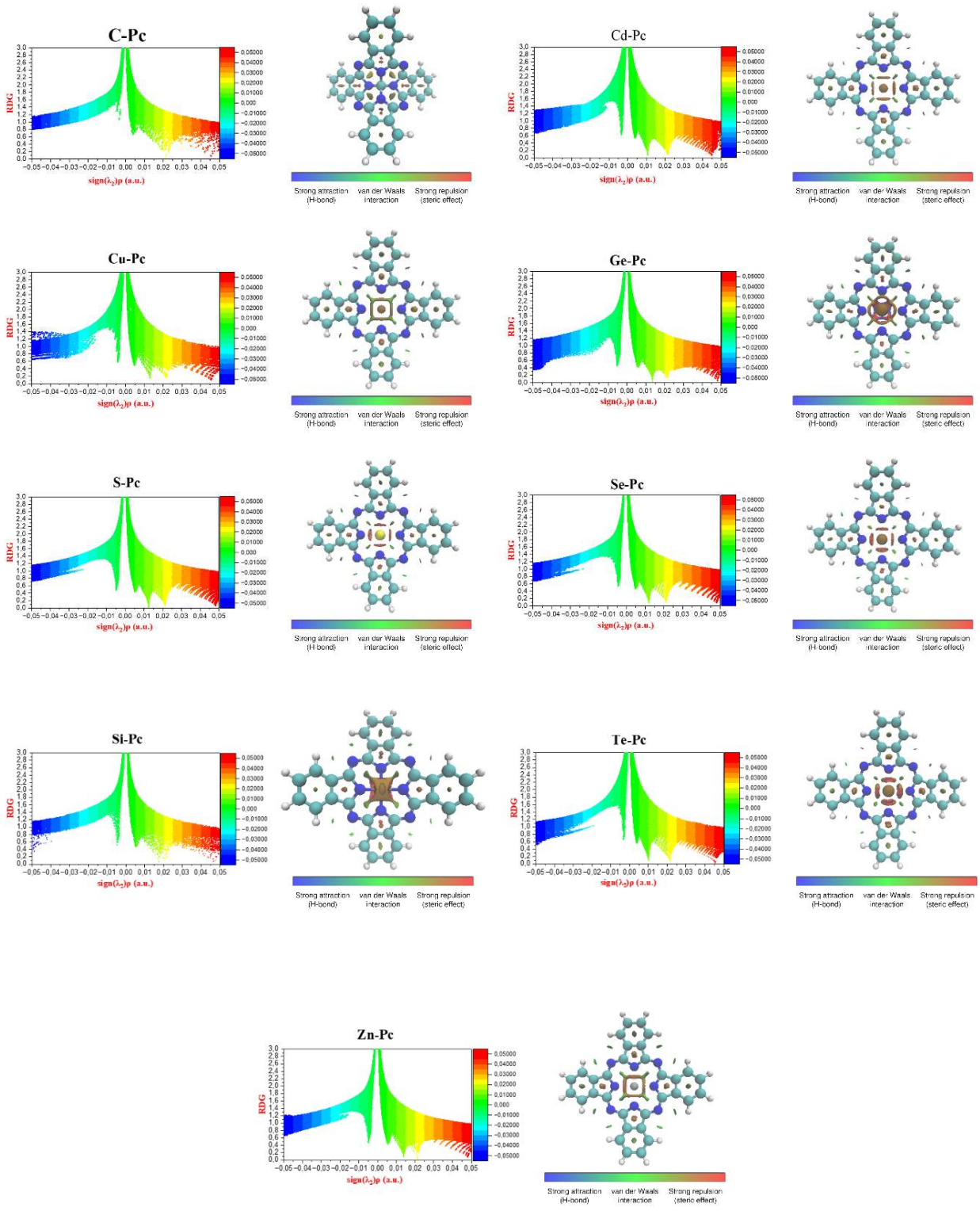


Fig.7. 2D RDG scatter plots and NCI isosurfaces of the studied HTMs.

3.7. Mulliken charge

Atomic charges can affect several characteristics of a molecular system, such as its electronic structure, dipole moment, acid–base behavior, molecular polarizability, and electrostatic potential surfaces. Analysis of atomic charges using the Mulliken method [46] is one of the most common population analyses. It helps distribute the electron density or wavefunction among the atoms in order to determine atomic charges and bonds [47], [48]. We studied Mulliken charges to better understand the distribution of electronic charges in the different phthalocyanines as shown in Figure 8. We observed that the four coordinated nitrogen atoms possess the most negative Mulliken charges, whereas the central atoms exhibit positive charges. In other words, the central atoms receive electron donation from the four nitrogen atoms,

corresponding to charge transfer from the ligand to the center in the studied phthalocyanines ((a) Zn-Pc, (b) Cu-Pc, (c) Cd-Pc, (d) C-Pc, (e) Si-Pc, (f) Ge-Pc, (g) S-Pc, (h) Se-Pc, and (i) Te-Pc.) [49], [50], [51]

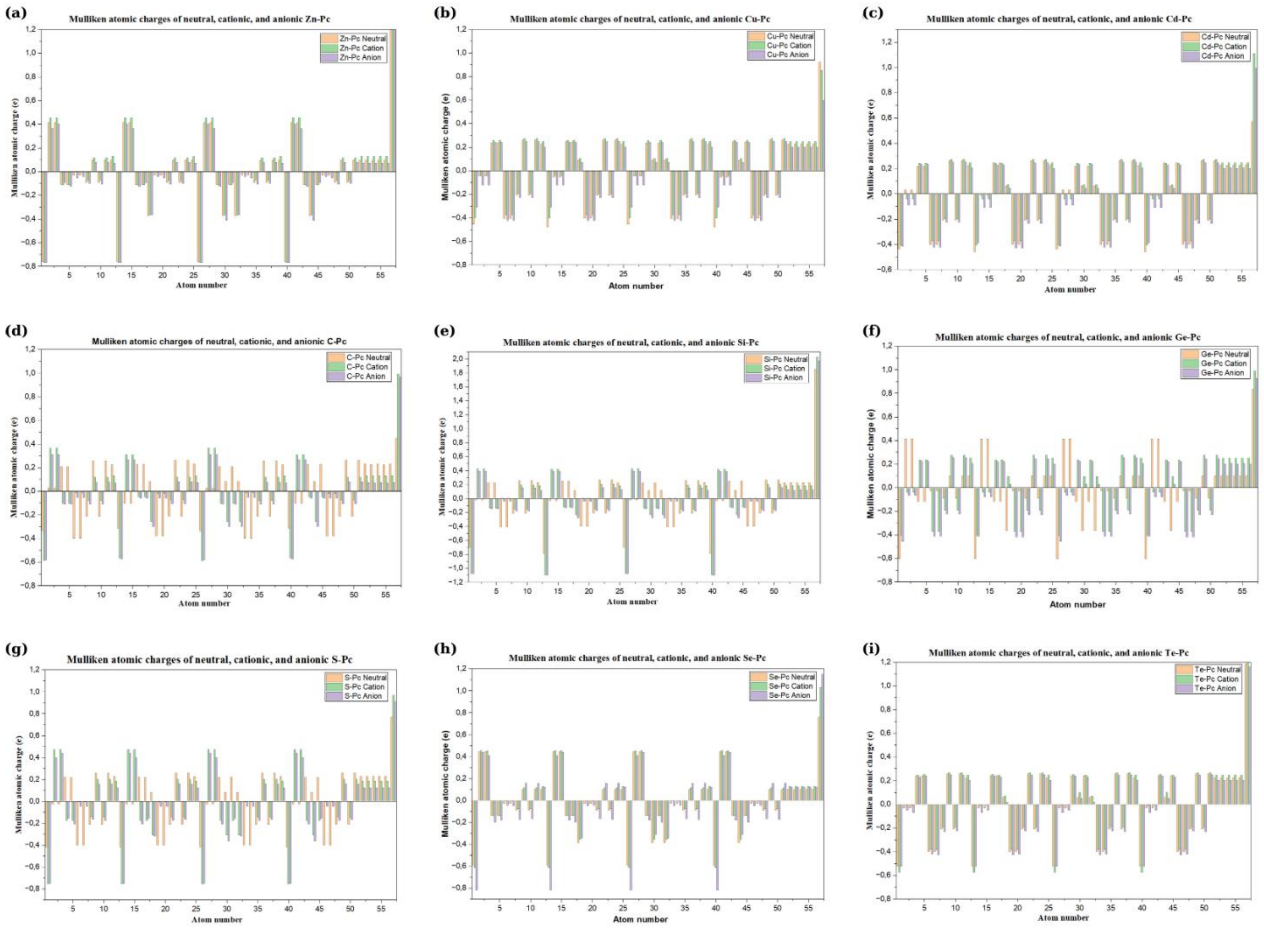


Fig.8. Mulliken atomic charge distributions of the investigated HTMs in their neutral, cationic, and anionic states: (a) Zn-Pc, (b) Cu-Pc, (c) Cd-Pc, (d) C-Pc, (e) Si-Pc, (f) Ge-Pc, (g) S-Pc, (h) Se-Pc, and (i) Te-Pc, calculated at the B3LYP/LANL2DZ level.

3.8 Density of States Evaluation

The density of states (DOS) and overlap population density of states (OPDOS) are useful tools for analyzing the respective contributions of different fragments to the formation of the HOMO and LUMO orbitals [52], [53]. They also provide details on the percentage distribution of Mulliken charges in each part of the molecule [54]. We noted that, for all the compounds analyzed, the C–H skeleton curve closely follows the TDOS, highlighting that the electronic structure is mainly influenced by the conjugated carbon macrocycle [55], [56]. These results are shown in Figure 9.We also observe that the contribution of the central atom is generally limited and concentrated in specific energy regions, indicating that replacement of the center affects only certain electronic states [57]. The main contributions are particularly pronounced for Cu-Pc, Cd-Pc, Si-Pc, Ge-Pc, and Te-Pc, whereas they remain negligible for Zn-Pc and C-Pc. Overall, these results indicate that the C–H skeleton essentially controls the density of states, whereas the central atom offers the possibility of modulating certain electronic levels.

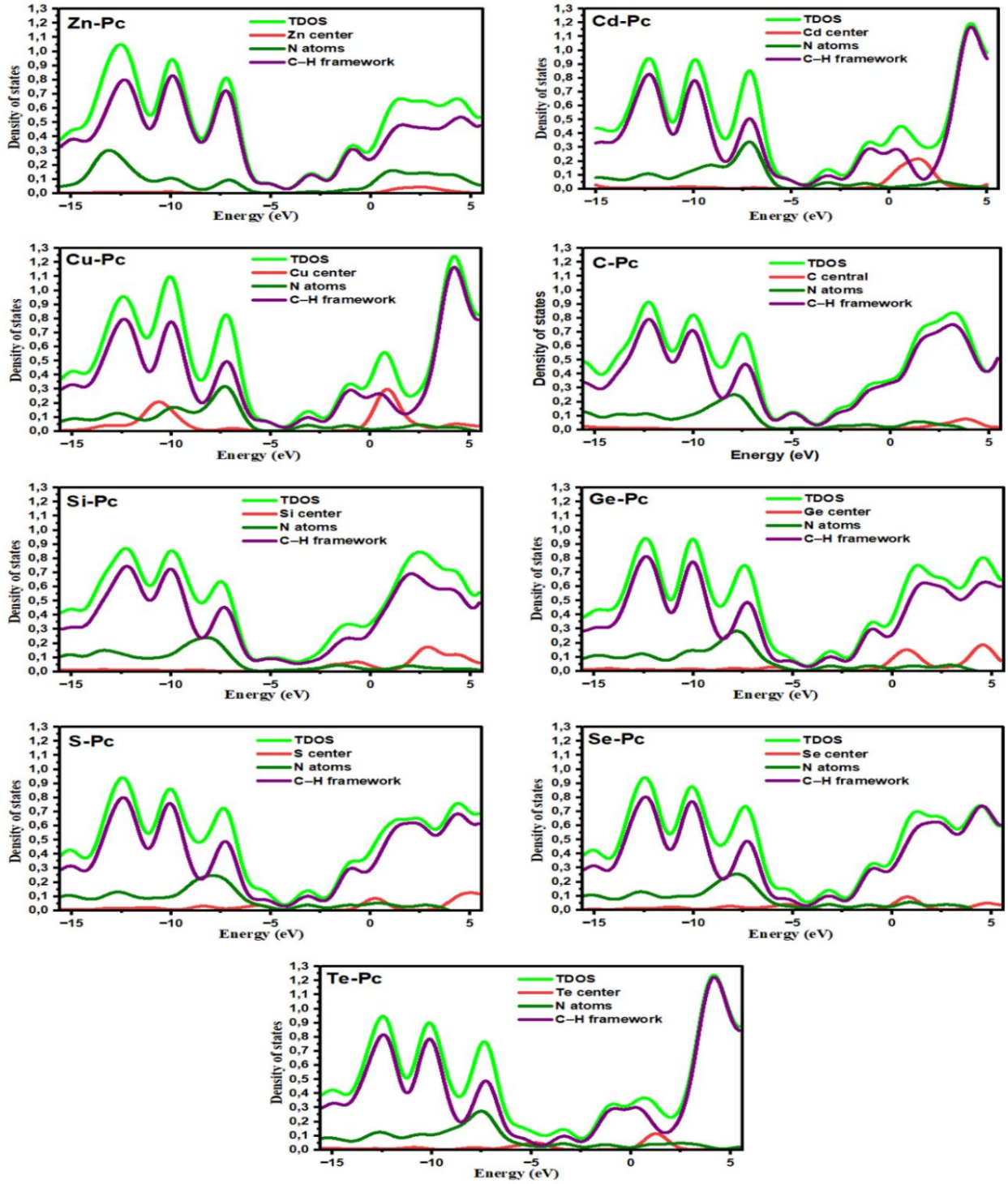


Figure 9. Density of states (DOS) plots of the nine studied phthalocyanine derivatives: Zn-Pc, Cu-Pc, Cd-Pc, C-Pc, Si-Pc, Ge-Pc, S-Pc, Se-Pc, and Te-Pc.

3.9 Absorption spectra

According to Figure 10, which presents the UV–Visible absorption spectra of the nine molecules studied, Zn-Pc, Cu-Pc, and Cd-Pc exhibit the most intense absorption bands. This trend is consistent with their energy-gap values and electronic transitions[58]. In contrast, Ge-Pc, S-Pc, and Se-Pc exhibit bands of intermediate intensity. C-Pc and Si-Pc exhibit less intense bands, whereas Te-Pc exhibits very weak absorption in the visible region and a main band shifted toward the near-infrared. Thus, all the molecules absorb in the visible region, with varying intensities, except for Si-Pc, C-Pc, and Te-Pc, which are transparent in the visible region. The latter are therefore the most favorable candidates for use as HTM materials in perovskite solar cells.

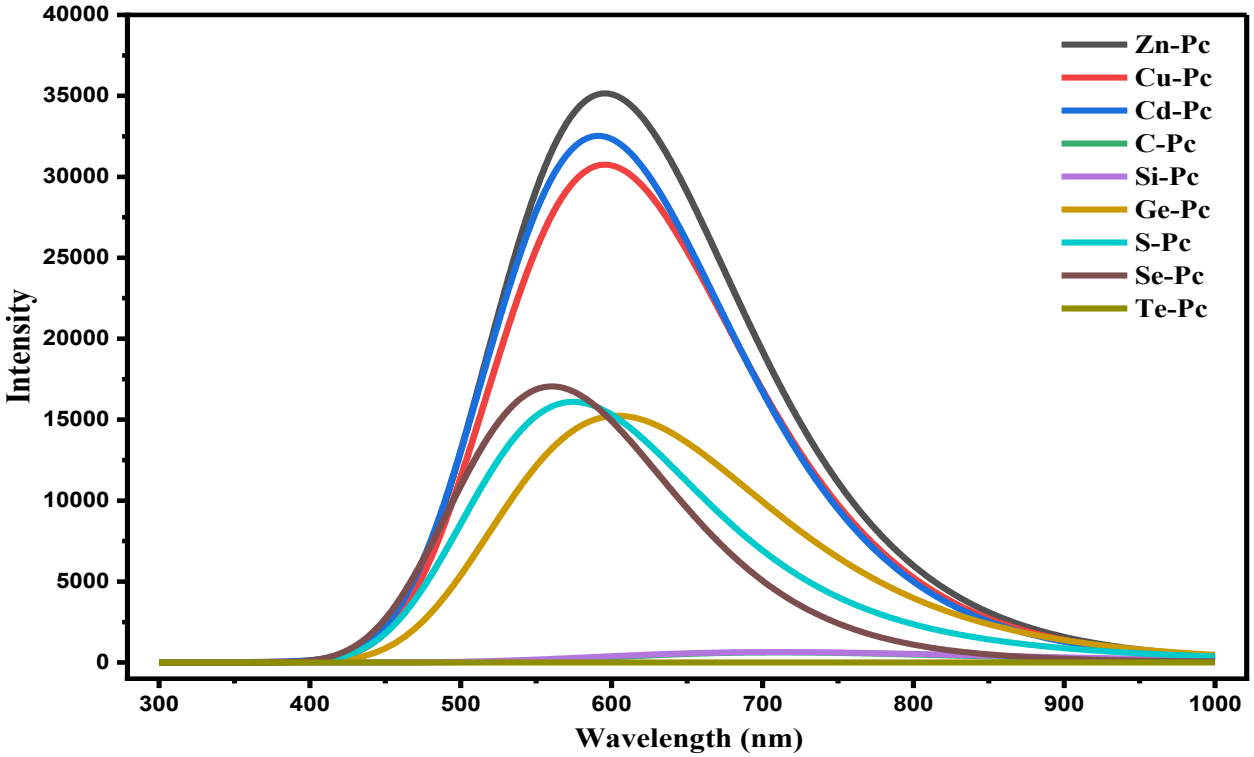


Fig. 10. UV–Visible absorption spectra of the nine phthalocyanine derivatives studied (Zn-Pc, Cu-Pc, Cd-Pc, C-Pc, Si-Pc, Ge-Pc, S-Pc, Se-Pc, and Te-Pc) obtained by TD-DFT/B3LYP/LANL2DZ calculations.

4. Conclusions

In conclusion, substituting the central atom significantly modifies the structural, electronic, and optical properties of the studied phthalocyanine-based hole-transport materials (HTMs). All the studied HTMs exhibit favorable properties. However, C-Pc, Si-Pc, and Te-Pc stand out as promising candidates for hole transport in perovskite solar cells due to their favorable electronic properties and advantageous absorption characteristics.

Funding

The authors received no funding for this work.

[1] N. Shahzad, S. A. S. Chatha, R. Hussain, S. Hussain, J. Iqbal, et M. Adnan, « Impact of End-capped Acceptor Modification in Anthanthrone-Based D-π-A Type Donor Materials for Organic and as Hole Transporting Materials for Perovskite Solar Cells », *J. Fluoresc.*, vol. 35, nº 11, p. 10499-10524, avr. 2025, doi: 10.1007/s10895-025-04309-8.

[2] I. M. Abdellah, E. Yildirim, et A. El-Shafei, « Low-cost novel X-shaped hole transport materials for efficient perovskite solar cells: Molecular modelling of the core and schiff base effects on photovoltaic and photophysical properties », *Mater. Chem. Phys.*, vol. 296, p. 127188, févr. 2023, doi: 10.1016/j.matchemphys.2022.127188.

[3] F. Rezaei et A. Mohajeri, « Molecular designing of triphenylamine-based hole-transporting materials for perovskite solar cells », *Sol. Energy*, vol. 221, p. 536-544, juin 2021, doi: 10.1016/j.solener.2021.04.055.

[4] Carmen Coppola, Rossella Infantino, Alessio Dessì, Lorenzo Zani, Maria Laura Parisi, Alessandro Mordini, Gianna Reginato, Riccardo Basosi, and Adalgisa Sinicropi, « *DFT* and *TDDFT* investigation of four triphenylamine/phenothiazine-based molecules as potential novel organic hole transport materials for perovskite solar cells », *Mater. Chem. Phys.*, vol. 278, p. 125603, févr. 2022, doi: 10.1016/j.matchemphys.2021.125603.

[5] H. Ashassi-Sorkhabi et P. Salehi-Abar, « Design of two novel hole transport materials via replacing the core of spiro-OMeTAD with tetrathiafulvalene and tetraazafulvalene for application in perovskite solar cells », *Sol. Energy*, vol. 173, p. 132-138, oct. 2018, doi: 10.1016/j.solener.2018.07.047.

[6] M. Adnan, H. Naz, M. Hussain, Z. Irshad, R. Hussain, et H. W. Darwish, « Development of Dopant-Free N,N′-Bicarbazole-Based Hole Transport Materials for Efficient Perovskite Solar Cells », *Int. J. Mol. Sci.*, vol. 25, nº 23, p. 13117, déc. 2024, doi: 10.3390/ijms252313117.

[7] D. Meng, J. Xue, Y. Zhao, E. Zhang, R. Zheng, et Y. Yang, « Configurable Organic Charge Carriers toward Stable Perovskite Photovoltaics », *Chem. Rev.*, vol. 122, nº 18, p. 14954-14986, sept. 2022, doi: 10.1021/acs.chemrev.2c00166.

[8] Hui-Seon Kim, Chang-Ryul Lee, Jeong-Hyeok Im, Ki-Beom Lee, Thomas Moehl, Arianna Marchioro, Soo-Jin Moon, Robin Humphry-Baker, Jun-Ho Yum, Jacques E. Moser, Michael Grätzel, and Nam-Gyu Park, « Lead iodide perovskite sensitized all-solid-state submicron thin film mesoscopic solar cell with efficiency exceeding 9% », *Sci. Rep.*, vol. 2, p. 591, 2012, doi: 10.1038/srep00591.

[9] M. M. Lee, J. Teuscher, T. Miyasaka, T. N. Murakami, et H. J. Snaith, « Efficient hybrid solar cells based on meso-superstructured organometal halide perovskites », *Science*, vol. 338, nº 6107, p. 643-647, nov. 2012, doi: 10.1126/science.1228604.

[10] « Best Research-Cell Efficiency Chart | Photovoltaic Research | NLR ». Consulté le: 3 août 2026. [En ligne]. Disponible sur: https://www.nlr.gov/pv/cell-efficiency

[11] R. Chetri, D. Devadiga, et A. T N, « A review on 4,4′-Dimethoxydiphenylamines bearing carbazoles as hole transporting materials for highly efficient perovskite solar cell », *Sol. Energy*, vol. 278, p. 112791, août 2024, doi: 10.1016/j.solener.2024.112791.

[12] N. S. Babu et I. O. Riwa, « DFT and TD-DFT studies of 1,3,5-Tris (dipheny1amino) benzene derivatives based hole transport materials: application for perovskite solar cells », *Opt. Quantum Electron.*, vol. 54, nº 6, p. 389, juin 2022, doi: 10.1007/s11082-022-03776-8.

[13] M. Orio, D. A. Pantazis, et F. Neese, « Density functional theory », *Photosynth. Res.*, vol. 102, nº 2, p. 443-453, déc. 2009, doi: 10.1007/s11120-009-9404-8.

[14] R. Dennington, T. A. Keith, and J. M. Millam, GaussView, Version 6.0, Semichem Inc., Shawnee Mission, KS, USA, 2016.

[15] S. Naqvi et A. Patra, « Hole transport materials for perovskite solar cells: A computational study », *Mater. Chem. Phys.*, vol. 258, p. 123863, janv. 2021, doi: 10.1016/j.matchemphys.2020.123863.

[16] R. G. Parr, S. R. Gadre, et L. J. Bartolotti, « Local density functional theory of atoms and molecules », *Proc. Natl. Acad. Sci. U. S. A.*, vol. 76, nº 6, p. 2522-2526, juin 1979, doi: 10.1073/pnas.76.6.2522.

[17] Z. Liu, X. Zhang, Y. Zhang, et J. Jiang, « Theoretical investigation of the molecular, electronic structures and vibrational spectra of a series of first transition metal phthalocyanines », *Spectrochim. Acta. A. Mol. Biomol. Spectrosc.*, vol. 67, nº 5, p. 1232-1246, août 2007, doi: 10.1016/j.saa.2006.10.013.

[18] Waqas Akram, Waqar Ali Zahid, Shaimaa A.M. Abdelmohsen, Meznah M. Alanazi, Ismail Hossain, Abraham Elmushyakhi, and Javed Iqbal, « Tailoring electronic structure and charge transport in thiophene-based hole transport materials: An end-capping acceptor strategy for efficient perovskite solar cells », *J. Phys. Chem. Solids*, vol. 182, p. 111596, nov. 2023, doi: 10.1016/j.jpcs.2023.111596.

[19] Shuxia Tao, Ines Schmidt, Geert Brocks, Junke Jiang, Ionut Tranca, Klaus Meerholz, and Selina Olthof, « Absolute energy level positions in tin- and lead-based halide perovskites », *Nat. Commun.*, vol. 10, juin 2019, doi: 10.1038/s41467-019-10468-7.

[20] Mohamed Jabha, Mohammed El Mesky, Hicham Zgueni, Nabil Amri, Yousef Youssefi, M'barek Azdouz, Driss Chebabe, Mohamed Azrour, El Houssine Mabrouk, Mohamed Znini, and Ahmad Oubair, « The intelligence way of economical synthesis strategies of an N-alkylcarbazole », *Struct. Chem.*, vol. 35, nº 2, p. 605-614, avr. 2024, doi: 10.1007/s11224-023-02214-z.

[21] L. Ueno, C. Jayme, L. Silva, E. Pereira, S. Oliveira, et A. E. Da Hora Machado, « Photophysics and spectroscopic properties of zinc phthalocyanine revisited using quantum chemistry », *J. Braz. Chem. Soc.*, vol. 23, p. 2237-2247, déc. 2012, doi: 10.1590/S0103-50532012001200013.

[22] J. Mack et M. J. Stillman, « Band Deconvolution Analysis of the Absorption and Magnetic Circular Dichroism Spectral Data of ZnPc(-2) Recorded at Cryogenic Temperatures », Consulté le: 7 août 2026. [En ligne]. Disponible sur: https://dx.doi.org/10.1021/j100020a015

[23] D. Pop, B. Winter, W. Freyer, W. Widdra, et I. V. Hertel, « Photoelectron Spectroscopy on Thin Films of Extended Zinc Porphyrazines », Consulté le: 7 août 2026. [En ligne]. Disponible sur: https://dx.doi.org/10.1021/jp046576i

[24] Z. Zhang, W. Hu, J. Cui, R. He, W. Shen, et M. Li, « Theoretical insights into the effect of a conjugated core on the hole transport properties of hole-transporting materials for perovskite solar cells », *Phys. Chem. Chem. Phys.*, vol. 19, nº 36, p. 24574-24582, sept. 2017, doi: 10.1039/c7cp04754a.

[25] N. Shahzad, S. A. S. Chatha, J. Iqbal, et S. Hussain, « Exploration of end-capped acceptors engineering in bis-3,4-ethylenedioxythiophene-based highly efficient near-infrared (NIR) organic molecules for perovskite and organic solar cells », *Struct. Chem.*, avr. 2026, doi: 10.1007/s11224-026-02786-6.

[26] Nabeel Shahzad, Muhammad Ishaq, Aqsa Laraib, Tazeem Fatima, Rida Fatima, Waqas Akram, and Javed Iqbal, « Optimizing Charge Transport Properties of Dithieno[3,2-b:2′,3′-d] Pyrrole-Based Hole Transport Materials for Perovskite Solar Cells: a DFT Study », *J. Fluoresc.*, vol. 36, nº 1, p. 183-201, oct. 2025, doi: 10.1007/s10895-025-04565-8.

[27] Waqar Ali Zahid, Muhammad Fiaz Ahmad, Waqas Akram, Ibrahim A. Shaaban, Mohammed A. Assiri, Abraham Elmushyakhi, and Javed Iqbal, « Probing the Effect of Acceptor Moiety Engineering in Carbazole-Based Hole-Transporting Materials for Efficient Perovskite Solar Cells », *Adv. Theory Simul.*, vol. 6, nº 11, p. 2300495, nov. 2023, doi: 10.1002/adts.202300495.

[28] Sabir Ali Siddique, Muhammad Arshad, Sabiha Naveed, Muhammad Yasir Mehboob, Muhammad Adnan, Riaz Hussain, Babar Ali, Muhammad Bilal Ahmed Siddique, and Xin Liu, « Efficient tuning of zinc phthalocyanine-based dyes for dye-sensitized solar cells: a detailed DFT study », *RSC Adv.*, vol. 11, nº 44, p. 27570-27582, 2021, doi: 10.1039/D1RA04529F.

[29] J. S. Murray et P. Politzer, « Molecular electrostatic potentials and noncovalent interactions », *WIREs Comput. Mol. Sci.*, vol. 7, nº 6, p. e1326, 2017, doi: 10.1002/wcms.1326.

[30] Muhammad Bilal Ahmed Siddique, Riaz Hussain, Sabir Ali Siddique, Muhammad Yasir Mehboob, Zobia Irshad, Javed Iqbal, and Muhammad Adnan, « Designing Triphenylamine-Configured Donor Materials with Promising Photovoltaic Properties for Highly Efficient Organic Solar Cells », *ChemistrySelect*, vol. 5, p. 7358-7369, juill. 2020, doi: 10.1002/slct.202001989.

[31] N. Shahzad, R. Fatima, H. Etabti, S. A. Shahid Chatha, et J. Iqbal, « Quantum design and investigation of dibenzo[g,p]chrysene-based hole transport materials for efficient perovskite solar cells », *Sol. Energy*, vol. 301, p. 113980, nov. 2025, doi: 10.1016/j.solener.2025.113980.

[32] Guichuan Zhang, Francis R. Lin, Feng Qi, Thomas Heumüller, Andreas Distler, Hans-Joachim Egelhaaf, Ning Li, Philip C. Y. Chow, Christoph J. Brabec, Alex K.-Y. Jen, and Hin-Lap Yip, « Renewed Prospects for Organic Photovoltaics », *Chem. Rev.*, vol. 122, nº 18, p. 14180-14274, sept. 2022, doi: 10.1021/acs.chemrev.1c00955.

[33] D. Chakraborty et P. K. Chattaraj, « Conceptual density functional theory based electronic structure principles », *Chem. Sci.*, vol. 12, nº 18, p. 6264-6279, 2021, doi: 10.1039/D0SC07017C.

[34] T. Ma, K. Inoue, H. Noma, K. Yao, et E. Abe, « Ionization potential studies of organic dye adsorbed onto TiO2 electrode », *J. Mater. Sci. Lett.*, vol. 21, p. 1013-1014, juill. 2002, doi: 10.1023/A:1016008623732.

[35] F. Zanjanchi et J. Beheshtian, « Natural pigments in dye-sensitized solar cell (DSSC): a DFT-TDDFT study », *J. Iran. Chem. Soc.*, vol. 16, p. 795-805, nov. 2018, doi: 10.1007/s13738-018-1561-2.

[36] W. Yang et R. G. Parr, « Hardness, softness, and the fukui function in the electronic theory of metals and catalysis. », *Proc. Natl. Acad. Sci.*, vol. 82, nº 20, p. 6723-6726, oct. 1985, doi: 10.1073/pnas.82.20.6723.

[37] A. Tanrıverdi et U. Yildiko, « Investigation of Theoretical Properties of Axially Disubstituted Silicon (iv) Phthalocyanine Compound by Computational Chemistry », *Int. J. Chem. Technol.*, vol. 9, p. 25-35, juin 2025, doi: 10.32571/ijct.1569679.

[38] M. Privado, P. de la Cruz, P. Malhotra, G. D. Sharma, et F. Langa, « Influence of the dipole moment on the photovoltaic performance of polymer solar cells employing non-fullerene small molecule acceptor », *Sol. Energy*, vol. 221, p. 393-401, juin 2021, doi: 10.1016/j.solener.2021.04.049.

[39] K. Altun, U. Yildiko, A. Tanrıverdi, et I. Cakmak, « Structural and spectral properties of 4-(4-(1-(4-Hydroxyphenyl)-1-phenylethyl)phenoxy)phthalonitrile: Analysis by TD-DFT method, ADME analysis and docking studies », *Int. J. Chem. Technol.*, vol. 5, p. 147-155, déc. 2021, doi: 10.32571/ijct.1004065.

[40] Aleksandr S. Kazachenko, Feride Akman, Hafedh Abdelmoulahi, Noureddine Issaoui, Yuriy N. Malyar, Omar Al-Dossary, and Marek J. Wojcik, « Intermolecular hydrogen bonds interactions in water clusters of ammonium sulfamate: FTIR, X-ray diffraction, AIM, DFT, RDG, ELF, NBO analysis », *J. Mol. Liq.*, vol. 342, p. 117475, nov. 2021, doi: 10.1016/j.molliq.2021.117475.

[41] N. Shanmugapriya, V. Balachandran, B. Revathi, B. Narayana, Vinutha V. Salian, K. Vanasundari, and C. Sivakumar, « Quantum chemical calculation, performance of selective antimicrobial activity using molecular docking analysis, RDG and experimental (FT-IR, FT-Raman) investigation of 4-[{2-[3-(4-chlorophenyl)-5-(4-propan-2-yl) phenyl)-4, 5-dihydro- 1H-pyrazol-1-yl]-4-oxo-1, 3- thiazol-5(4H)-ylidene} methyl] benzonitrile », *Heliyon*, vol. 7, nº 7, p. e07634, juill. 2021, doi: 10.1016/j.heliyon.2021.e07634.

[42] B. Gassoumi, F.E. Ben Mohamed, M.E. Castro, F.J. Melendez, A. Karayel, L. Nouar, F. Madi, H. Ghalla, S. Özkınalı, V.I. Kovalenko, R. Ben Chaabane, and H. Ben Ouada, « In silico exploration of O-H…X2+ (X = Cu, Ag, Hg) interaction, targeted adsorption zone, charge density *iso*-surface, O-H proton analysis and topographic parameters theory for calix[6]arene and calix[8]arene as model », *J. Mol. Liq.*, vol. 334, p. 116127, juill. 2021, doi: 10.1016/j.molliq.2021.116127.

[43] M. T. Alotaibi, « Noncovalent interaction stabilizes the 2, 4-Dinitrophenylhydrazone Derivatives over g-C3N4 surface to enhance optical properties: synthesis, characterization, and DFT investigation », *J. Mol. Struct.*, vol. 1214, p. 128192, 2020.

[44] R. A. Boto, J.-P. Piquemal, and J. Contreras-García, « (PDF) Revealing strong interactions with the reduced density gradient: a benchmark for covalent, ionic and charge-shift bonds ». Consulté le: 27 août 2026. [En ligne]. Disponible sur: https://www.researchgate.net/publication/321036955_Revealing_strong_interactions_with_the_reduced_density_gradient_a_benchmark_for_covalent_ionic_and_charge-shift_bonds

[45] X. An, Y. Kang, et G. Li, « The Interaction between Chitosan and Tannic acid Calculated Based on the Density Functional Theory », *Chem. Phys.*, vol. 520, déc. 2018, doi: 10.1016/j.chemphys.2018.12.009.

[46] Z. S. Şahin, H. Şenöz, H. Tezcan, et O. Büyükgüngör, « Synthesis, spectral analysis, structural elucidation and quantum chemical studies of (E)-methyl-4-[(2-phenylhydrazono)methyl]benzoate », *Spectrochim. Acta. A. Mol. Biomol. Spectrosc.*, vol. 143, p. 91-100, mai 2015, doi: 10.1016/j.saa.2015.02.032.

[47] A. A. El-Saady, N. Roushdy, A. A. M. Farag, M. M. El-Nahass, et D. M. Abdel Basset, « Exploring the molecular spectroscopic and electronic characterization of nanocrystalline Metal-free phthalocyanine: a DFT investigation », *Opt. Quantum Electron.*, vol. 55, nº 7, p. 662, mai 2023, doi: 10.1007/s11082-023-04877-8.

[48] M. A. M. El-Mansy, M. S. El-Bana, et S. S. Fouad, « On the spectroscopic analyses of 3-Hydroxy-1-Phenyl-Pyridazin-6(2H)one (HPHP): A comparative experimental and computational study », *Spectrochim. Acta. A. Mol. Biomol. Spectrosc.*, vol. 176, p. 99-105, avr. 2017, doi: 10.1016/j.saa.2016.12.040.

[49] S. Aydogdu, G. Yasa Atmaca, A. Erdoğmuş, et A. Hatipoglu, « Synthesis of a new Zn-phthalocyanine, photophysical, photochemical, and sono-photochemical properties and DFT studies », *Polyhedron*, vol. 256, p. 116989, juill. 2024, doi: 10.1016/j.poly.2024.116989.

[50] K. J. Hamam et M. I. Alomari, « A study of the optical band gap of zinc phthalocyanine nanoparticles using UV–Vis spectroscopy and DFT function », *Appl. Nanosci.*, vol. 7, nº 5, p. 261-268, juin 2017, doi: 10.1007/s13204-017-0568-9.

[51] M. Ağırtaş, D. Güngördü Solğun, et U. Yildiko, « Synthesis, theoretical DFT analysis, photophysical and photochemical properties of a new zinc phthalocyanine compound », *Inorg. Nano-Met. Chem.*, vol. 54, p. 301-311, févr. 2022, doi: 10.1080/24701556.2022.2034005.

[52] Waqas Akram, Waqar Ali Zahid, Lamia Abu El Maati, Reem Altuijri, Ismail Hossain, Mohammed Salim Akhter, and Javed Iqbal, « Engineering push–pull structural versatility in highly functional carbazole-based hole transporting materials design for efficient perovskites solar devices », *J. Photochem. Photobiol. Chem.*, vol. 444, p. 114991, 2023.

[53] R. Fatima, J. Iqbal, S. Bibi, et M. Yaseen, « Exploring Acceptor Modification in Helicene-Phenylamine-Based Small Molecules for Organic and Perovskite Solar Cells », *Energy Technol.*, vol. 12, nº 2, p. 2301019, 2024, doi: 10.1002/ente.202301019.

[54] P. Mahalingavelar, « How End-Capped Acceptors Regulate the Photovoltaic Performance of the Organic Solar Cells: A Detailed Density Functional Exploration of Their Impact on the A–D−π–D–A Type Small Molecular Electron Donors », *Energy Fuels*, vol. 36, nº 4, p. 2095-2107, févr. 2022, doi: 10.1021/acs.energyfuels.1c04272.

[55] M.-S. Liao et S. Scheiner, « Electronic structure and bonding in metal phthalocyanines, Metal=Fe, Co, Ni, Cu, Zn, Mg », *J. Chem. Phys.*, vol. 114, nº 22, p. 9780-9791, juin 2001, doi: 10.1063/1.1367374.

[56] Fabrizio Evangelista, Vincenzo Carravetta, Giovanni Stefani, Branislav Jansik, Michele Alagia, Stefano Stranges, and Alessandro Ruocco, « Electronic structure of copper phthalocyanine: An experimental and theoretical study of occupied and unoccupied levels », *J. Chem. Phys.*, vol. 126, p. 124709-124709, mars 2007, doi: 10.1063/1.2712435.

[57] Q. Zhou, Z.-F. Liu, T. J. Marks, et P. Darancet, « Electronic Structure of Metallophthalocyanines, MPc (M = Fe, Co, Ni, Cu, Zn, Mg) and Fluorinated MPc », *J. Phys. Chem. A*, vol. 125, nº 19, p. 4055-4061, mai 2021, doi: 10.1021/acs.jpca.0c10766.

[58] M. Ammari, M. Jabha, M. Yaakoubi, S. Kharchouf, A. Elalaoui, et E. H. Mabrouk, « Optimization of ZnPc and TPA-ZnPc phthalocyanines as hole transport materials to improve the performance of perovskite solar cells », *Mod. Electron. Mater.*, vol. 12, nº 1, p. 17-24, avr. 2026, doi: 10.3897/j.moem.12.1.166784.